*J. Mater. Environ. Sci. 7 (3) (2016) 907-914*
*ISSN : 2028-2508*
*CODEN: JMESCN*



# Effect of heat treatment on $TiO_2$ thin films properties

**A. El Fanaoui[1, 2*], A. Taleb[3,4*], E. El Hamri[1], L. Boulkaddat[1], H. Kirou[1], L. Atourki[1], A. Ihlal[1] and K. Bouabid[1]**

[1] *Laboratory Materials and Renewable Energies (LMRE), Ibn Zoh University, Dep. Physics, Faculty of Science BP8106, Hay Dakhla, 80000 Agadir, Morocco.*

[2]*Ecole Supérieure de Technologie de Guelmim (ESTG), Avenue Abou Maachar Al Balkhi, B.P. : 1317, 81000 Guelmim, Morocco.*

[3]*Institut de Recherche de Chimie Paris, CNRS – Chimie ParisTech, 11 rue Pierre et Marie Curie, 75005 Paris, France.*

[4] *Sorbonne Universités,UPMC Univ Paris 06, F-75005, Paris*

*Received 26 Aug 2015, Revised 28 Nov 2015, Accepted 13 Dec 2015*

*[*]Corresponding Authors. E-mail: elfanaouiaha@yahoo.fr; abdelhafed.taleb@upmc.fr ; Tel: (+212661286908)*

## Abstract

The aim of this study was to investigate the influence of the annealing temperature on the structural and optical properties of $TiO_2$ thin films, deposited by chemical bath deposition method (CBD) onto glass substrates. The X-ray diffraction (XRD) experiments show that the well-known anatase phase was observed for some annealing temperature. The best conditions of crystallization were found upon annealing at temperatures higher than 400 °C in the air. The surface morphology of the deposited films characterized by the Field-Emission Gun Scanning Electron Microscope (FEGSEM) consists of granular texture with a clear identified grain at the surface. The size of the grains is more than 100 nm and increases with annealing temperature. The UV-Vis-NIR spectroscopy shows that our films exhibit a high value of optical transmission which is around 80%. The indirect band gap of the deposited films was found to range between 3.17 and 3.44 eV depending on the annealing temperature. The Urbach energy increases with the annealing temperature.

*Keywords*: Anatase, band gap, chemical bath deposition, rutile, titanium dioxide.

## Introduction

Much attention has been paid these last decades to the study of titanium dioxide. In this respect, particular interest has been attached to the environmental applications of such material that is gaining in popularity day after day. Indeed, extensive studies and investigations are being conducted for various applications, explicitly photo-induced water splitting [1], dye-sensitized solar cell [2], environmental purification [3], many other electric, optical and catalytic applications [4–9] and nanoparticle $TiO_2$ materials have been used in various electrochemical and photoelectrochemical applications [10, 11]. Furthermore, $TiO_2$ has become an attractive electrode material for electrochemical sensors and biosensors applications, due to its good biocompatibility, high conductivity and low cost [12, 13]. The chemical and physical properties of the prepared materials depend strongly on the method used for their fabrication. Many approaches have been tested for the preparation of $TiO_2$ thin films, including electron beam evaporation [14–16], magnetron sputtering [17], mist plasma evaporation [18], pulsed laser deposition [19], self-assembly process [20], laser chemical vapor depositing [21, 22], cathodic electrodeposition [23-24], sol gel [25] metal organic chemical vapor deposition [26]. Non vacuum methods are very attractive and seem to be preferred since they do not require a high capital investment. Among, these techniques, sol gel (spin-coating and dip-coating) are some of the most popular approaches: They are simple,

cost effective, easy to scale-up and suitable for a large area processing. In our previous works [27, 28], we have demonstrated the high crystalline quality of $TiO_2$ thin films prepared with sol gel method.
In this contribution, we present our recent results on $TiO_2$ thin films prepared with another traditional method frequently used and identified as cost effective and highly efficient; chemical bath deposition. The influence of annealing temperature on the structural and optical properties will be presented and discussed.

## 2. Experimental procedure

For the synthesis of $TiO_2$ thin films, the peroxo-titanium precursor was prepared in the aqueous acidic medium by mixing $TiOSO_4$ powder and $H_2O_2$ with constant stirring for 25 min to get a red clear solution [23]. The obtained solution was kept in the bath at room temperature with constant stirring. The glass substrate was cleaned in an ultrasonic bath with an acetone and ethanol solution, then it is rinsed with bidistilled water and finally purged with nitrogen gas. The glass substrates were immersed vertically in the solution. After 12h deposition time, the substrates were withdrawn from the solution, sufficiently rinsed with the bidistilled water and purged with nitrogen gas at room temperature (25°C). The films were then dried at 100 °C for 1 h and subsequently annealed at 350, 400, 450 and 500 °C in air during 1 h.
The optical measurements were performed using a Cary 50 (Varian) UV-Vis-NIR spectrophotometer equipped with unpolarized light and operating at normal incidence in the wavelength range from 300 nm to 850 nm. A glass substrate cleaned with the same procedure described above was used as reference.
The morphological investigations of the prepared films were achieved with a high-resolution Ultra 55 Zeiss FEG scanning electron microscope (FEGSEM) operating at an acceleration voltage of 10 KV. The film thickness was measured with a Dektak 6 M stylus profiler.
Energy dispersive X-ray spectroscopy (EDS) analysis was used to determine the chemical composition of the prepared films and realized in FEGSEM using a PGT spirit energy dispersive spectrometry system (EDS).
The crystalline structure was determined by an X-ray diffractometer (Siemens D5000 XRD unit) in 2θ range from 20° to 80° by 0.07° $s^{-1}$ increasing steps operating at 40 KV accelerating voltage and 40 mA current using CuK$\alpha$ radiation source with λ= 1.5406Å.

## 3. Results and discussion

First, it is worth noting that all the prepared films were firmly adhesive on the substrate. No peel off was noticed from the substrates after annealing. The thickness of the prepared $TiO_2$ films was roughly about 200 nm (Figure 1(a)).

### *3.1. Structural and morphological characterizations*

Figure 1(b) shows the XRD patterns of $TiO_2$ films annealing at different temperatures 350, 400, 450 and 500°C. As seen, $TiO_2$ film annealed at 350°C was amorphous. The crystallization process begins after annealing at 400°C. Indeed, XRD patterns of $TiO_2$ films obtained after annealing at 400, 450 and 500°C for 1 h in air, present an obvious diffraction peak at 25.3° assigned to (101) crystallographic plane of anatase. These results show that the crystallization of $TiO_2$ improves by increasing the annealing temperature.
The grain sizes of $TiO_2$ films were calculated by the Scherrer equation (1) [29]:

$$D = \frac{0.89\lambda}{(\beta_{obs}^2 - \beta_{ins}^2)^{1/2}\cos\theta_{hkl}} \qquad \textbf{(1)}$$

Where D is the crystal dimension perpendicular to the reflecting plane, λ = 1.5406Å is the wavelength of CuKα radiation source, $\theta_{hkl}$ is the angle of bragg diffraction, $\beta_{ins}$ is the instrumental broadening, $\beta_{obs}$ is the full width at half maximum (fwhm) of the diffraction peak and $(\beta^2_{obs} - \beta^2_{ins})^{1/2}$ is the fwhm of the diffraction peak after correcting for broadening caused by the diffractometer. The obtained grain size from the calculation using Eq. 1 for the annealed films at temperatures of 400, 450 and 500°C are respectively 33 nm, 40 nm and 47 nm.

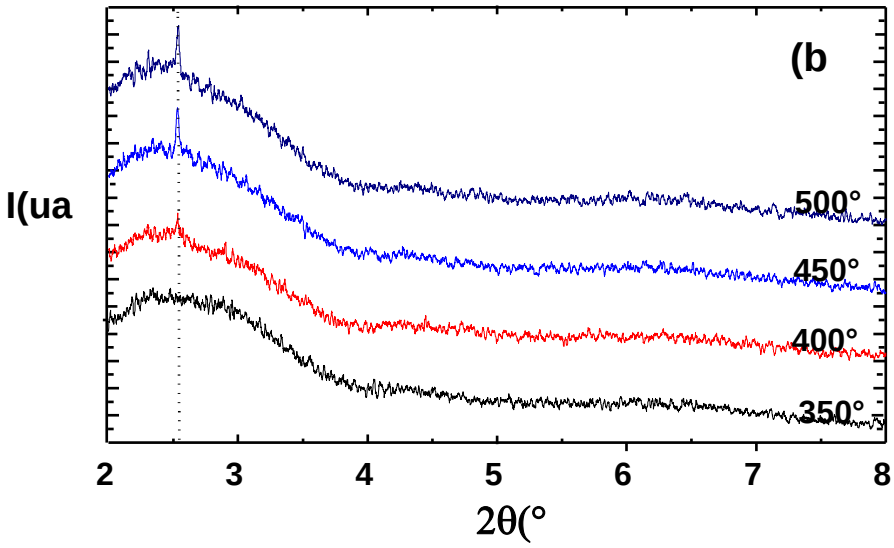


**Figure 1:** (a) The film thickness measurement using stylus profiler, (b) XRD pattern of $TiO_2$ films annealed at different temperatures: 350, 400, 450 and 500°C.

At room pressure, $TiO_2$ occurs in three crystalline polymorphs: rutile (tetragonal, a=0.4593nm, c=0.2959 nm), anatase (tetragonal, a=0.3785 nm, c=0.9514 nm), and brookite (orthorhombic, a=0.5436 nm, b=0.9166 nm, c=0.5135 nm) [25-26]. The anatase and brookite phases are known to be thermodynamically less stable than the rutile phase, so they can easily be converted into the other phases at high temperatures [25-26]. Only anatase and rutile, which possess tetragonal structures, have been observed in thin film up to now [25-26]. Anatase $TiO_2$ is a low temperature stable phase, which transforms into rutile structure at high temperatures above 800°C [30, 31]. In addition, amorphous $TiO_2$ films are often observed when the substrate temperature during deposition is low [32]. The band structure calculations revealed that rutile and anatase $TiO_2$ have respectively direct and indirect band gap [33]. Although a wide range of band-gap energies have been reported for both rutile and anatase $TiO_2$ samples by optical measurements, anatase $TiO_2$ is known to have higher band-gap energy than that of rutile $TiO_2$ [33-35].

In Figure 2 (a)–(d) we present the FEGSEM images of the $TiO_2$ thin films annealed at different temperatures of 350, 400, 450 and 500°C.

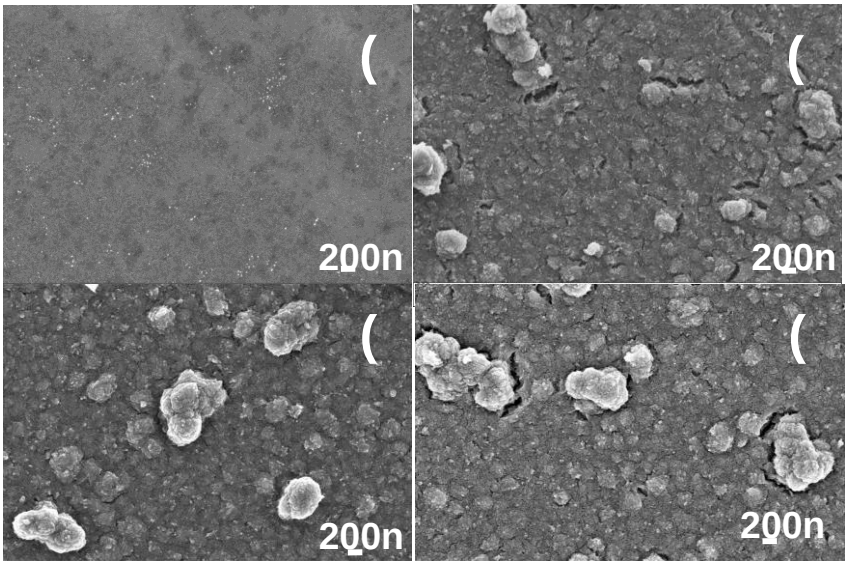


**Figure 2:** SEM images of $TiO_2$ thin films annealed at different temperatures: (a) 350°C, (b) 400°C, (c) 450°C and (d) 500°C.

The films cover the whole substrate and show a crack free, rough surface, no pinholes and granular texture with clearly identified grain at the surface. It is also seen that the sizes of the grains are more than 100 nm and increase with annealing temperature. The results of the XRD investigations reported above, revealed grain sizes less than 100 nm determined from the FEGSEM images. This can be explained by the fact that the grains consist of a set of domains in which size is ranging from 33 nm to 47 nm. The energy dispersive X-ray (EDX) analysis in Figure 3 reveals the existence of Ti and O elements on the surface of annealed films as well as other chemical species coming from the glass substrate. Unfortunately no quantitative analysis was performed on our samples.

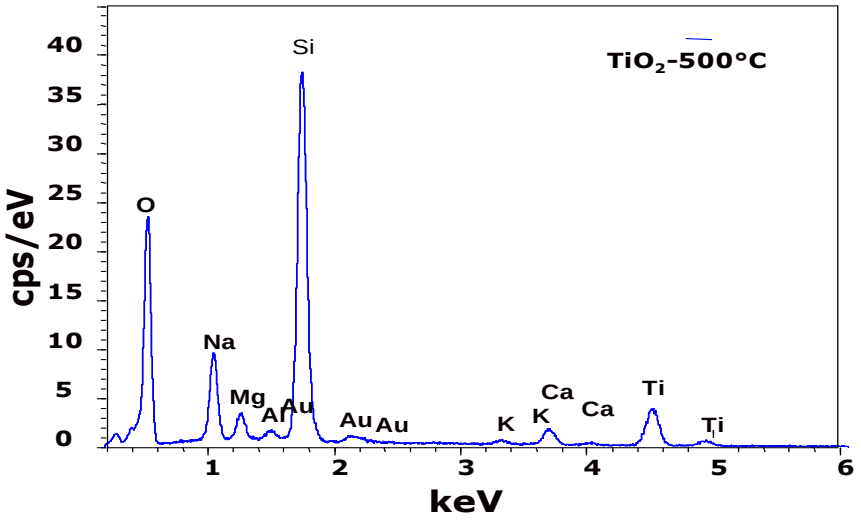


**Figure 3:** The energy dispersive X-ray (EDX) analysis of $TiO_2$ thin film annealed at temperature of 500°C.

*3.2. Optical properties*

Figure 4 shows the optical transmission spectra of $TiO_2$ films annealed at different temperatures of 350, 400, 450 and 500°C. As it is seen, the optical transmission of $TiO_2$ films in the visible wavelength region is enhanced to nearly 80% by increasing annealing temperature. This is attributed to the increase of structural homogeneity and the decrease of the defect density [36].

The optical band gap of $TiO_2$ film can be determined from the sharply falling transmission region. According to Tauc equation below [37], the absorption coefficient has the following energy dependence (equation (2)):

$$\alpha = \frac{B(h\nu - E_g)^{\frac{1}{r}}}{h\nu} \qquad (2)$$

Where B is a constant which does not depend on hυ, and for most semiconductors it is in the range of $10^5$–$10^6$ $cm^{-1}$ $eV^{\frac{r-1}{r}}$ [38]; r is the power coefficient whose value indicates the type of predominant electronic transitions; it takes the following values of 1/2, 2, 3/2 or 3 respectively for allowed direct, allowed indirect, forbidden direct and forbidden indirect electronic transitions [39, 40]. The best fit of $(\alpha h\upsilon)^r$ versus hυ gives the value of r=1/2 in the case of our annealed films and that of the most oxide.

The band gap is determined by plotting, $(\alpha h\upsilon)^r$ versus, hυ, and extrapolating the linear region of the plot toward low energies. This graphic method is approximate for determining semiconductors band gap because it assumed that the refractive index is constant in the energy range considered [41]. By neglecting the reflectivity, the absorption coefficient ($\boldsymbol{\alpha}$) can be determined from the $TiO_2$ film transmission, T, using equation (3) below:

$$\alpha = \frac{\ln(\frac{1}{T})}{d} \qquad (3)$$

Where d is the thickness of the film [42].

In Figure 5 we present a comparison of the $(\alpha.h\upsilon)^{1/2}$ versus hυ plots of $TiO_2$ films annealed at different temperatures. The results denote that the band gap can be tuned by varying the annealing temperature. However

lower optical band gap can be obtained for higher annealing temperature. The indirect optical band gap values ($E_g$) are 3.44; 3.37; 3.30 and 3.17 eV for $TiO_2$ films annealed at 350, 400, 450 and 500°C, respectively. The allowed indirect transitions have been previously found for different Anatase $TiO_2$ films [43, 44].

The inset in Figure 5 presents the dependence of the optical band gap of $TiO_2$ films on the annealing temperature. From the graph, it is clear that the optical band gap increases almost linearly with the reduction of the annealing temperature. The optical band gap of $TiO_2$ film is obviously affected by the defects and the film crystallinity [44]. From Figure 5 and based on the XRD results of the structural analysis, in terms of the grain size gains with the increasing of the annealing temperature, it is apparent that the optical band gap decreases with the increase of grain size and thus the decrease of defects density. Similar results were observed by other authors and explained by the fact that free electrons are trapped into the defects and the grain boundaries [45].

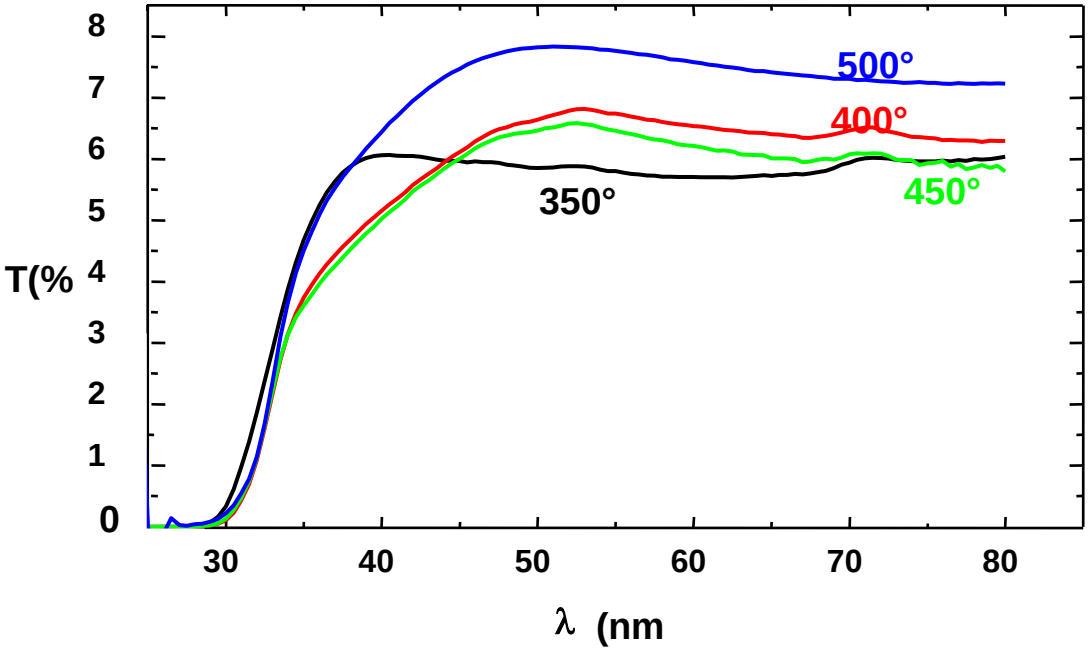


**Figure 4:** The Optical transmission spectra of $TiO_2$ thin films annealed at different temperatures: 350, 400, 450 and 500°C.

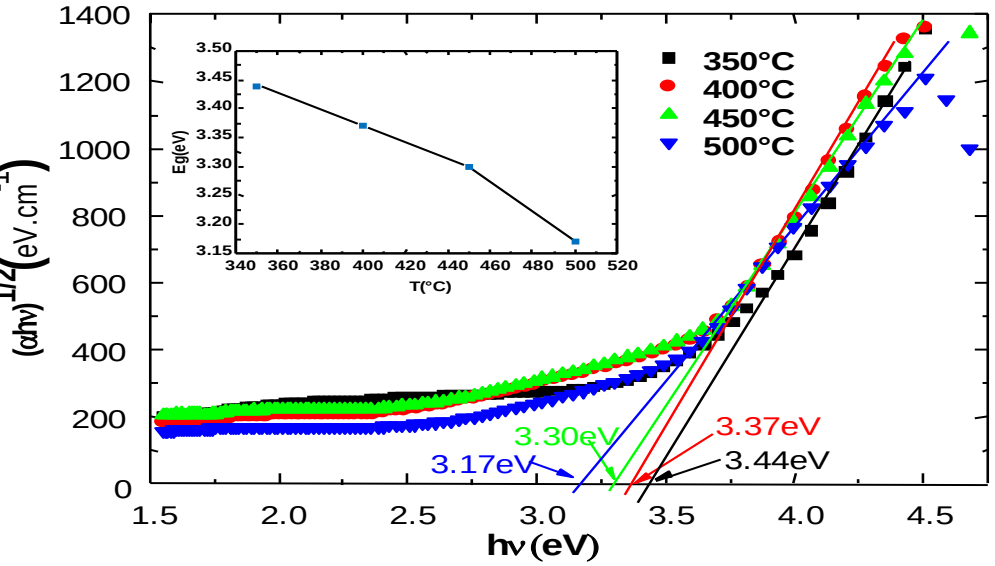


**Figure 5:** The comparison of the $(\alpha.h\upsilon)^{1/2}$ versus hυ plots of $TiO_2$ thin films annealed at different temperatures. The dependence of $TiO_2$ film band gap on the annealing temperature is shown in the inset.

Urbach energy of samples is calculated by using the empirical Urbach rule given by equation (4) [46, 48]:

$$\alpha = \alpha_0 e^{\frac{E}{E_u}} \qquad (4)$$

Where α is the absorption coefficient, E is the photon energy and $E_u$ is the Urbach energy. For the calculation of Urbach energy, lnα is plotted against E. The reciprocal of the slope of linear portion, below optical band gap, gives the value of $E_u$ [47, 48]. The Urbach energy curves of entire samples are displayed in Fig. 4 and the values of $E_u$ at different temperatures are inserted in Table1. We notice that the width of Urbach tail increases with the film annealing temperature; this is most probably due to the decrease of order with the annealing temperature. Furthermore the observed high Urbach energy for $TiO_2$ annealed at 500°C is attributed to the presence of large number of oxygen vacancies in$TiO_2$ [49]. This interpretation is supported by many previous studies, in which impedance spectroscopy measurements are used to characterize the gas-sensing behavior of undoped titanium dioxide ($TiO_2$) polycrystalline thin films [50] and to show bistable resistive switching of anatase $TiO_2$ films [51]

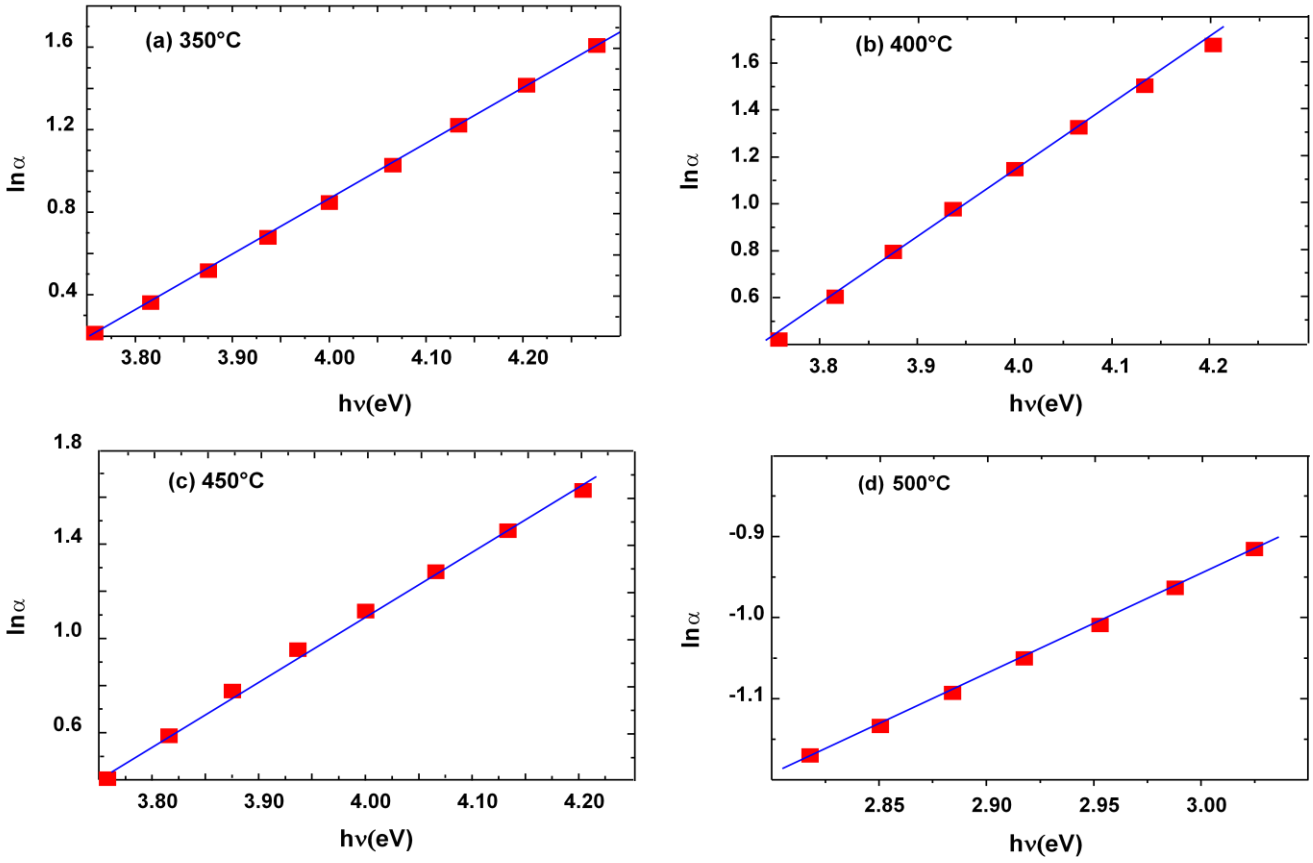


**Figure 6:** Determination of Urbach energy of $TiO_2$ thin films annealed at different temperatures.

**Table 1:** Urbach energy of $TiO_2$ thin films at different annealed temperatures.

| T(°C) | 350 | 400 | 450 | 500 |
|---|---|---|---|---|
| $E_u$(meV) | 373 | 350 | 361 | 806 |

## Conclusion

This study deals with the preparation and characterization of Anatase $TiO_2$ thin films, using a cost effective method: Chemical Bath Deposition. It has been shown that homogenous and firmly adhesive layers can be prepared easily. The obtained films consist on homogeneous granular surface with nano-sized particles of few tens of nanometers. Increasing annealing temperature has lead to the improvement of the crystalline quality of the films, the reduction of the band gap value and increase the urbach energy.

**Acknowledgments-**This work was partially supported by the CNRST/CNRS cooperation program.

## References

1. Yamakata A., Ishibashi T., Onishi H., *J. Mol. Catal. A: Chem*. 199 (2003) 85-94.
2. O'Regan B., Graetzel M., *Nature* 353(1991) 737-740.
3. Ikezawa S., Homyara H., Kubota T., Suzuki R., Koh S., Mutuga F., Yoshioka T., Nishiwaki A., Ninomiya Y., Takahashi M., Baba K., Kida K., Hara T., Famakinwa T., *Thin Solid Films* 386 (2001) 173-176.
4. Wang Y.L., Zhang K.Y., Van V.N., Souche D., Rivory J., *Thin Solid Films* 307 (1997) 38-42.
5. Mergel D., Buschendorf D., Eggert S., Grammes R., Samset B., *Thin Solid Films* 371 (2000) 218-224.
6. Nakataa K., Fujishima A., *Photochemistry Reviews* 13 (2012) 169-189.
7. Banakh O., Schnid P.E., Sanjines R., Levy F., *Surf. Coat. Technol* 151 (2002) 272-275.
8. Carrocci J. S., Mori R. Y., Guimarães O. L. C., Salazar R. F. 0., Oliveira M. C. F., Peixoto A. L. C., Filho H. J. I., *Engineering* 4 (2012) 746-760.
9. Ellouzi. I,. ELayazi. L,. Harir. M,. Schmitt. K. P., Laanab. L., Mountacer. H., El Hajjaji. S., *Physical and Chemical News* 75 (2015) 60-67
10. Wen D., Guo S., Wang Y., Dong S., *Langmuir* 26 (2010) 11401-11406.
11. Mandal S., Bhattacharyya A. J., *J. Chem. Sci. 124 (2012) 969–978.*
12. Fan Y., Lu H. T., Liu J. H., Yang C. P., Jing Q. S., Zhang Y. X., Yang X. K., Huang K. J., *Colloids Surfaces B 83 (2011) 78-82.*
13. *Li K., Zhu M., Zhang H., Zhao J., Int. J. Electrochem. Sci. 8 (2013) 4047 – 4054.*
14. Cevro M., Carter G., J. Phys. D, *Appl. Phys.* 28, (1995) 1962-1976.
15. Pulker H.K., *Thin Solid Films* 34 (1976) 343-347.
16. Wang F.X., Hwangbo C.K., Jung B.Y., Lee J.H., Park B.H., Kim N.Y., *Surf. Coat. Technol*. 201 (2007) 5367-5370.
17. Bhagwat S., Howson R.P., *Surf. Coat. Technol*. 111 (1999) 163-171.
18. Huang H., Yao X., *J. Cryst. Growth* 268 (2004) 564-567.
19. Garapon C., Champeaux C., Mugnier J., Panczer G., Marchet P., Catherinot A., Jacquier B., *Appl. Surf. Sci*. 96-98 (1996) 836-841.
20. Huang D., Xiao Z.D., Gu J.H., Huang N.P., Yuan C.W., *Thin Solid Films* 305 (1997) 110-115.
21. Watanabe A., Imai Y., *Thin Solid Films* 348 (1999) 63-68.
22. Sankapal B.R., Lux-Steiner M.C., Ennaoui A., *Appl. Surf. Sci*. 239 (2005) 165-170.
23. Natarajan C., Nogami G., *J. Eletcrochem. Soc*. 143 (1996) 1547-1570.
24. Karuppuchamy S., Nonomura K., Yoshida T., Sugiura T., Minoura H., *Solid State Ionics*. 151 (2002) 19-27.
25. Jung C.K., Bae I.S., Song Y.H., Kim T.K., Vlcek J., Musil J., Boo J.H., *Surf. Coat. Technol*. 200 (2005) 534-538.
26. Antunes R. A., Deoliveira M. C. L., Pillis M. F., *Int. J. Electrochem. Sci.* 8 (2013) 1487 – 1500.
27. El Fanaoui A., El Hamri E., Boulkaddat L., Ihlal A., Bouabid K., Laanab L., Taleb A., Portier X., *Int J*

*Hydrogen Energy*. 36 (2011) 4130-4133.
28. Bouabid K., Ihlal A., Amira Y., Sdaq A., Assabane A., Ait-Ichou Y., Outzourhit A., Ameziane E. L., Nouet G., *Ferroelectrics* 372 (2008) 69-75.
29. B. D. Cullity, Elements of X-ray Diffraction, second Ed., *Addison Wesley*, (1978).
30. Wiggins M.D., Neison M.C., Aita C. R., *J. Vac. Sci. Technol. A.* 14 (1996) 772-776.
31. Okimura K., Shibata A., Maeda N., Tachibana K., *Jpn. J. Appl. Phys*. 34 (1995) 4950-4955.
32. Williams L.M., Hess D.W., *J. Vac. Sci. Technol.* 1 (1983) 1810-1819.
33. Mo S.D., Ching W.Y., *Phys. Rev. B.* 51 (1995) 13023-13032.
34. Jellison Jr G.E., Boatner L.A., Budai J.D., Jeong B.S., Norton D.P., *J. Appl. Phys.* 93 (2003) 9537-9541.
35. Tang H., Levy F., Berger H., Schmid P.E., *Phys. Rev. B.* 52 (1995) 7771-7774.
36. Alam M.J., Cameron D.C., *Thin Solid Films* 377 (2000) 455-459.
37. Tauc J.C., Optical Properties of Solids, North-Holland, *Amsterdam* (1972) 372.
38. Domaradzki J., *Thin Solid Films* 497 (2006) 243-248.
39. Mott N.F., Davis E.A., Electronic Processes in Non-Crystalline Materials, Second ed., *Clarendon Press, Oxford* (1979)
40. Tauc J., Menth A., *J. Non-Cryst. Solids*. 8 (1972) 569-585.
41. Yang C., Fan H., Xi Y., Chen J., Li Z., *Applied Surface Science* 254 (2008) 2685-2689.
42. Kane J., Schweizer H.P., *Thin Solid Films* 29 (1975) 155-163.
43. Hasan M.M., Haseeb A.S.M.A., Saidur R., Masjuki H. H., Hamdi M., *Optical Materials* 32 (2010) 690-695.
44. Landmann M., Rauls E., Schmidt W.G., *J. Phys. Condens. Matter*. 24 (2012) 195503-195509.
45. Yang C., Fan H., Xi Y., Chen J., Li Z., *Appl. Surf. Sci*. 254 (2008) 2685-2689.
46. Natsume Y., Sakata H., Hirayama T., *Phys. Stat. Sol. (a)* 148 (1995) 485-495.
47. Boubaker K., *Eur. Phys. J. Plus.* 126 (2011) 10-14.
48. Choudhury B., Borah B., Choudhury A., *Photochem. Photobiol*. 88 (2012) 257-264.
49. Choudhury B., Choudhury A., *Physica E*. 56 (2014) 364–371.
50. Ponce M.A., Parra R., Savu R., Joanni E., Bueno P.R., Cilense M., Varela J.A., Castro M.S., *Sensors and Actuators* B 139 (2009) 447–452.
51. Jeong D. S., Schroeder H., Waser R., *Applied Physics Letters* 89 (2006) 082909.